

Surface roughness and residual stress evolution in $\text{SiN}_x/\text{SiO}_2$ multilayer coatings deposited by reactive pulsed magnetron sputtering

CHUEN-LIN TIEN^{1,2*}, PO-WEI LEE¹, SHIH-CHIN LIN³, HONG-YI LIN²

¹Department of Electrical Engineering, Feng Chia University, Taichung, Taiwan

²Ph.D. Program of Electrical and Communications Engineering, Feng Chia University, Taichung, Taiwan

³Mechanical and Systems Research Lab, Industrial Technology Research Institute, Hsinchu, Taiwan

*Corresponding author: cltien@fcu.edu.tw

The surface roughness and residual stress behavior in two types of $\text{SiN}_x/\text{SiO}_2$ dielectric quarter-wave stacks was investigated experimentally. A reactive pulsed magnetron sputtering system was used to prepare the $\text{SiN}_x/\text{SiO}_2$ multilayer thin films. The results show that $\text{SiN}_x/\text{SiO}_2$ quarter-wave stack with a buffer layer of MgF_2 thin film can reduce the residual stress. The effect of aging on the residual stress in two quarter-wave stacks was also studied. We found that the residual stresses in both $\text{SiN}_x/\text{SiO}_2$ multilayer coatings are changed from a compressive state to a tensile stress state with increasing the aging time. The root mean square (RMS) surface roughness of $\text{MgF}_2/(\text{SiN}_x/\text{SiO}_2)^{22}$ and $(\text{SiN}_x/\text{SiO}_2)^{22}$ quarter-wave stacks are 2.23 ± 0.22 nm and 2.08 ± 0.20 nm, respectively.

Keywords: thin film, residual stress, quarter-wave stacks, surface roughness.

1. Introduction

Silicon nitride (SiN_x) films have been widely used in optical coatings as a high refractive index material [1]. Silicon nitride thin films can be used as antireflection coatings and passivation layers because they possess several attractive features [2], for example, high hardness, corrosion resistance, temperature resistance, thermal conductivity and insulation. The characteristic development of SiN_x thin film is an important issue for material applications [3–5]. Silicon dioxide (SiO_2) is the common low-refractive index layer material in oxide-based optical coatings for the spectral range of 250–2500 nm. SiO_2 is the low absorption material used in combination with high-index oxide layer coatings that operate in the ultraviolet (~ 200 nm) to near-infrared (~ 3 μm) regions.

SiO_2 can be used in combination with specific high-index layers to form multilayer structures. In general, optical interference coatings typically utilize alternating layers of high-refractive and low-refractive index materials with the precise thickness control of each layer.

The residual stress in thin film multilayers is a critical issue for the optical coatings. The residual stress may affect the durability and quality of the optical thin film components. If the film stress is too large, it will cause the thin film component failure or damage. The measurement and evaluation of the residual stress in thin films are needed. The residual stresses in multilayer films are not only related to the deposition technology, but also dependent on the effect of interlayer in film structure. The residual stress in the multilayer films is more complicated because the adjacent layers and the coating substrate should be taken into consideration [6]. In the past decades, many studies were carried out to show that different processing conditions will affect the residual stress values. Therefore, an accurate evaluation and controlling the residual stress become a significant work in thin film coatings. ENNOS [7] reported an empirical formula for predicting residual stress in multilayer thin films which based on single layer film. TINONE *et al.* [8] presented low stress multilayer films grown by varying the relative thickness of each layer and by adjusting the radio-frequency (RF) powers during film deposition. They showed that the RF power is an experimental parameter to be controlled in order to change film stresses and to obtain low stress multilayer films. However, these studies are focused on the residual stress of evaporated dielectric films and sputtered metal films. The goal of this work is to fabricate multilayer films with a low residual stress and specific spectral reflectance requirements. In order to reduce the residual stress in the multilayer films, an effective method was proposed to compensate the residual stress by adding a layer of tensile stress of the MgF_2 film to the sputtered $(\text{SiN}_x/\text{SiO}_2)^{22}$ multilayer stack. After thin film deposition, the residual stress is measured by a home-made Twyman–Green interferometer combined with the fast Fourier transform method [9, 10]. The aging effect of the two $(\text{SiN}_x/\text{SiO}_2)^{22}$ multilayer stacks on the residual stress over time is also discussed in this study.

2. Experiment

In this experiment, the multilayer film $(\text{SiN}_x/\text{SiO}_2)^{22}$ is alternately stacked by two dielectric materials, which are composed of a low refractive index material SiO_2 and a high refractive index material SiN_x , wherein each layer has an optical thickness of one-quarter wavelength (QW). The $(\text{SiN}_x/\text{SiO}_2)^{22}$ and $\text{MgF}_2/(\text{SiN}_x/\text{SiO}_2)^{22}$ quarter wave layers were prepared by a reactive pulsed magnetron sputtering system. The MgF_2 film as a buffer layer is prepared by a thermal evaporation technique. For the reactive pulsed magnetron sputtering, the vacuum system is a combination of a mechanical pump and a turbo-molecular pump. The target is a 99.999% pure silicon placed on a vertical sputtering gun. The size of the target is 182 mm × 62 mm × 6 mm, the distance from the target to the substrate is 70 mm, and the background pressure to be reached before

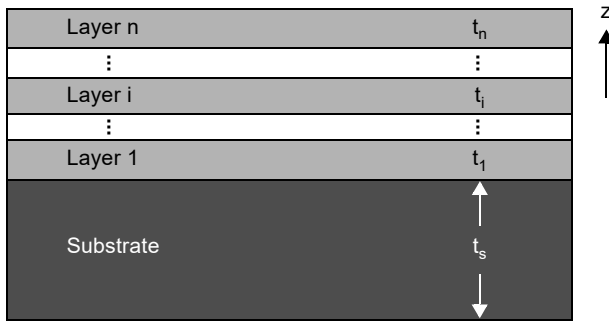


Fig. 1. Schematics of a multi-layered film structure.

each experiment is 8.0×10^{-6} Torr and BK7 glass substrates were placed on a rotatable substrate holder. Working pressure is about 1.07×10^{-3} Torr. The rotation speed of the substrate holder is 30 revolutions per minute (rpm). When a SiN_x film was deposited, argon (Ar) and nitrogen (N_2) were used as sputtering and reaction gases at flow rates of 20 and 12 sccm, respectively. The total working pressure of Ar and N_2 is 1.2×10^{-1} Pa. The flow rates of Ar and O_2 when depositing the SiO_2 film were 80 and 9 sccm, respectively. The working pressure is 2.4×10^{-1} Pa. The pulse charging and discharging time were 30 and 40 μs , respectively. The reactive pulsed magnetron sputtering was connected to a pulse controller and activated by a DC power supply. The DC power supply was set to a constant power mode of 550 W. The substrate temperature was heated to 100°C . Controlling the reactive gas through closed loop control stabilizes the stoichiometric ratio of the film to achieve high rate deposition. In order to provide some insights into the multilayer designs, a multi-layered film structure is schematically shown in Fig. 1, where n layers of film with individual thickness t_i are bonded sequentially to a substrate with thickness of t_s . The subscript i denotes the layer number for the thin film and is ranged from 1 to n with the layer 1 being the buffer-layer.

In this work, a home-made Twyman–Green interferometer was used to measure the residual stress of thin films. The optical setup for residual stress measurement is shown in Fig. 2. A He-Ne laser passing through a micro-objective and a pinhole, as a spatial filter, form a point source and then propagate through a collimating lens to form a plane wavefront. The wavefront is divided in amplitude by a beam splitter. A circular BK7 glass substrate (25.4 mm in diameter and 2.0 mm in thickness) was placed on a substrate holder and acts as a test plate. The reflected and transmitted beams travel to a reference plate and a test plate. After being reflected by both the reference plate and the tested substrate, two beams recombine to form interference fringes and travel toward a digital CCD camera. The interference pattern can be seen on a LCD monitor through the CCD camera. The captured interference images were analyzed by the fast Fourier transform (FFT) method [11]. The analyzed software based on the MATLAB software was used to determine the radius of curvature of the tested substrates. Finally, the residual stress of the thin film was calculated from the change of

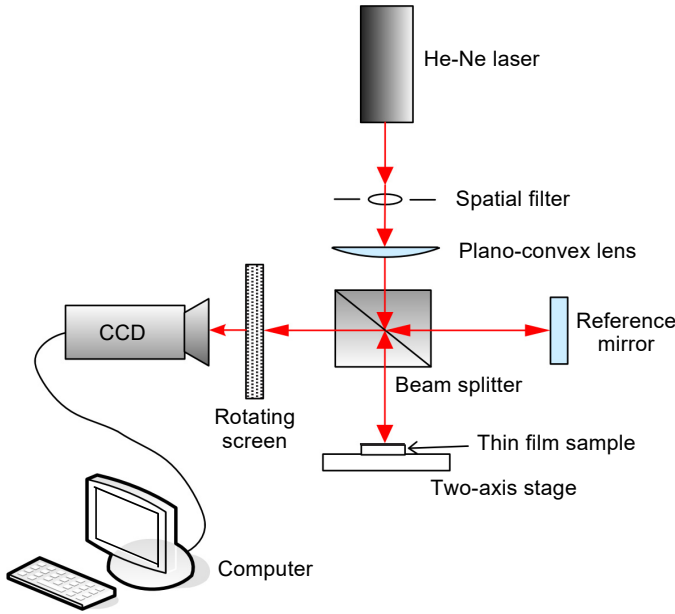


Fig. 2. Schematics of a film stress measurement system.

the radius of curvature of the substrate before and after coatings. Stoney formula was used to determine the residual stress [12, 13]. The modified Stoney formula is expressed as follows:

$$\sigma = \frac{E_s t_s^2}{6(1 - \nu_s) t_f} \left(\frac{1}{R_2} - \frac{1}{R_1} \right) \quad (1)$$

where σ is the residual stress in thin films; R_1 and R_2 are the radius of curvature before and after thin-film is deposited on a BK7 glass substrate. The BK7 glass substrates are single sided polished to a flatness of one wavelength. $E_s = 81$ GPa and $\nu_s = 0.208$ are the Young's modulus and the Poisson's ratio of the BK7 glass substrate, respectively; t_s is the thickness of the substrate and t_f ($t_f \ll t_s$) is the film thickness. The tensile residual stress is taken to be positive. Meanwhile, the compressive stress is taken to be negative.

The average residual stress of the multilayer film can be evaluated by the formula proposed by ENNOS [7]. The Ennos empirical formula is expressed as follows:

$$\sigma_{\text{total}} = \frac{\sigma_1 t_1 + \sigma_2 t_2 + \dots + \sigma_n t_n}{\sum_{i=1}^n t_i} = \frac{\sum_{i=1}^n \sigma_i t_i}{T_f} \quad (2)$$

where σ_i and t_i are the residual stress and film thickness of each layer of the coating, respectively. T_f is the total thickness of the multilayer coating. R is the change of the

radius of curvature before and after the multilayer coating. The average residual stress of the multilayer is weighted by the film thickness of each layer. The average residual stress of multilayer coatings can be simulated by self-developed MATLAB software, and the residual stress evolution can be used to understand the stress behavior in multilayer thin films.

In this work, the use of a buffer layer as a means of adjusting the residual stress in the multilayer coating was explored. Multilayers deposited using sputtering typically exhibit the presence of compressive stress behavior. The MgF_2 film has a low refractive index, and it has been confirmed that the MgF_2 film deposited by the thermal evaporation method exhibits a tensile film stress. Several analytical models have been developed to predict residual stresses in multilayer films on substrates [14, 15]. This analytical method will help to design a multilayer coating with lower residual stress. In the stress simulation, we set the stress data of the single-layer material to the initial value, and then input the design layer of the high-refractive-index material and the low-refractive-index material. The thickness is set to a quarter wavelength or a non-quarter wavelength. The total average stress can be evaluated by the self-developed MATLAB program [16]. We expect that the simulation method described herein for evaluating residual stress can be applied to reactive pulsed magnetron sputtering deposition, but needs to include other related effects for a complete understanding. Surface roughness was measured by a microscope interferometer associated with FFT and Gaussian filter. The configuration of the microscope interferometer is derived from a Michelson

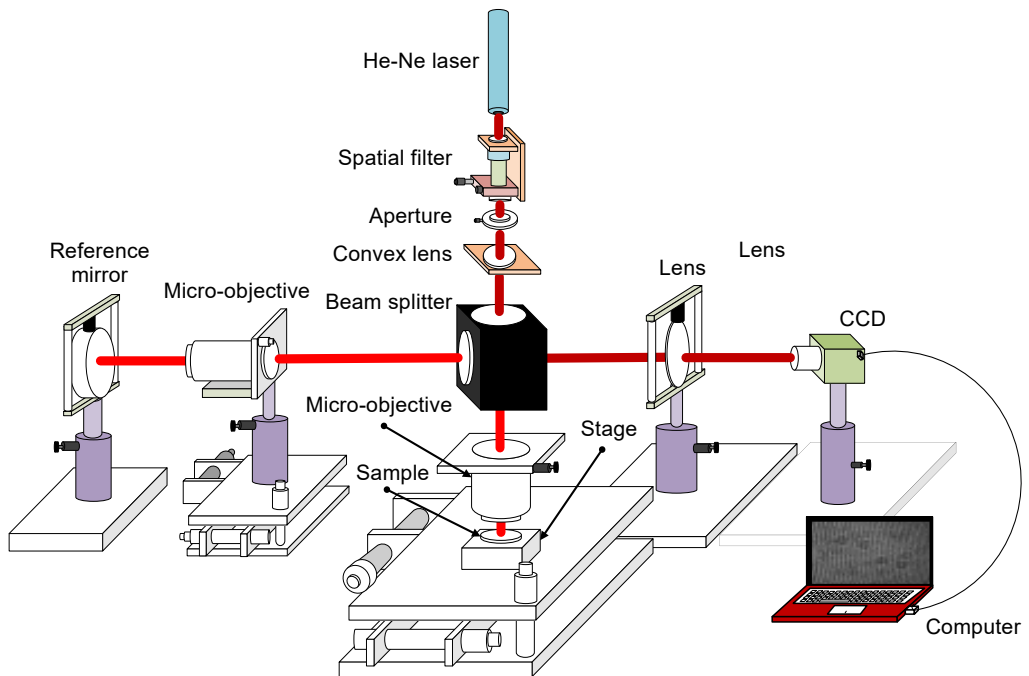


Fig. 3. Schematics of a surface roughness measurement system.

microscope interferometer. This system is not only equipped with a 50× microscope objective on a testing path but is equipped with the same microscope objective on a reference path. This arrangement has advantage to compensate for optical aberrations. The microscope interferometer measurement system is shown in Fig. 3. After reconstructing the film surface profile by the FFT method, using a Gaussian filter to remove the high-frequency signal and to acquire the roughness profile, the root mean square (RMS) and average roughness can be evaluated from the surface profile.

3. Results and discussion

Figure 4 shows that the multilayer film transmission spectra of two $\text{SiN}_x/\text{SiO}_2$ alternately stacked were measured by a Perkin–Elmer Lambda-900 optical spectrophotometer in the wavelength range from 250 to 2000 nm. The optical band stop filter was designed for the dual band-rejection wavelengths of 700–850 nm and 860–1060 nm, respectively. The average transmission outside the stop-band is about 85%. The total thickness of the film was measured by the α -step stylus profilometer (Surfcorder ET3000, Kosaka Laboratory Ltd., Japan).

In this study, the optical band-stop filter composed of multilayer stacks of alternating quarter-wave films of SiN_x and SiO_2 deposited by a reactive DC pulsed magnetron sputtering system on BK7 glass substrates. The stress value of SiN_x and SiO_2 single layer films were -210 and -204 MPa, respectively. A buffer layer of MgF_2 film was deposited by thermal evaporation with a tensile stress of 197 MPa, and then added to form a 45-layer $\text{MgF}_2/(\text{SiN}_x/\text{SiO}_2)^{22}$ quarter-wave (QW) stack.

For the residual stress, the prediction was simulated by a self-developed MATLAB program based on the Ennos empirical formula. Figure 5 shows 44 layers of the $(\text{SiN}_x/\text{SiO}_2)^{22}$ multilayer films, and the compressive residual stress is -91.27 MPa for the simulation and -11.38 MPa for the stress measurement. A 45-layer of alternating QW stack of SiN_x and SiO_2 , and an additional buffer layer of MgF_2 films is designed for a band-stop filter. The residual stress is -74.66 MPa for the simulation and

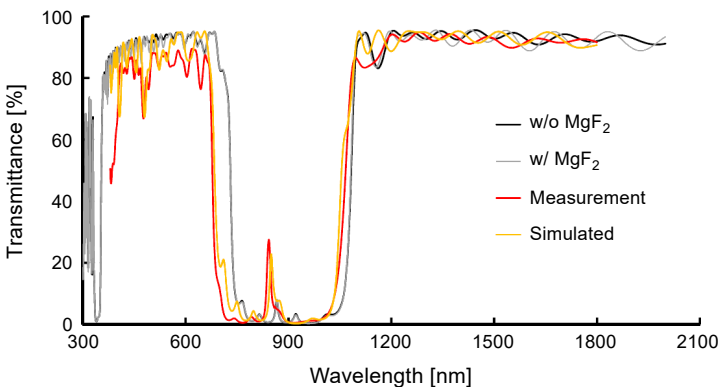


Fig. 4. Transmittance spectra of different multilayer stacks.

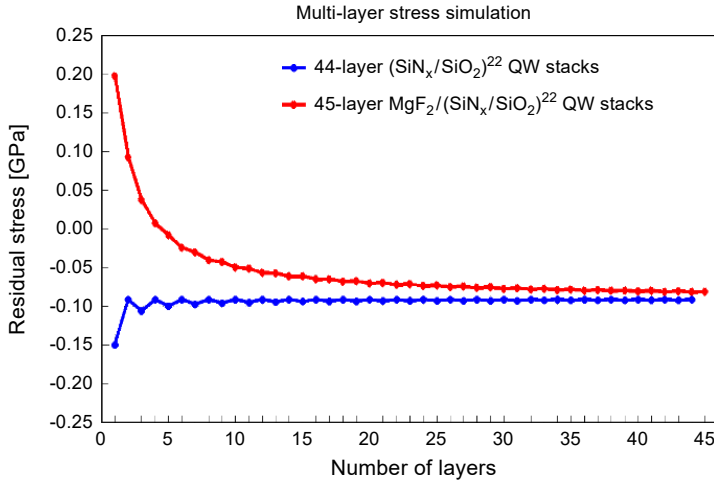


Fig. 5. Stress simulations of 44-layer and 45-layer quarter-wave stacks.

-8.43 MPa for the measurement. The difference between simulation and measurement value is mainly due to the Ennos formula which ignores the interface stress between the film layers. The stress on the interlayer surface is essentially controlled by the stress/strain of the interlayer. It is worth noting that the residual stress in 45 layers of the QW stack is less than that of 44-layer QW stack. It is owing to a MgF₂ film which in tensile state is added to the film stack and balances out the stress level of the multilayer and reduces the total residual stresses. Therefore, the goal of reducing the residual stress can be achieved.

The relationship between the stress evolution and the aging time of the two multi-layer designs is shown in Fig. 6. It shows the multilayer films of (SiN_x/SiO₂)²² QW stack, where the compressive stress is changed from -11.38 to -1.56 MPa. Fur-

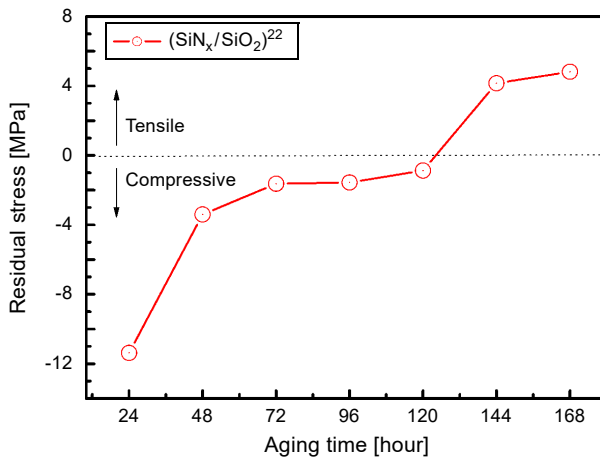


Fig. 6. Residual stress versus the aging time for (SiN_x/SiO₂)²² quarter-wave stack.

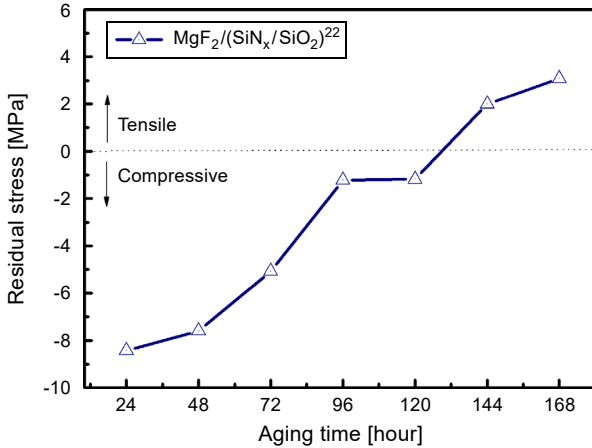
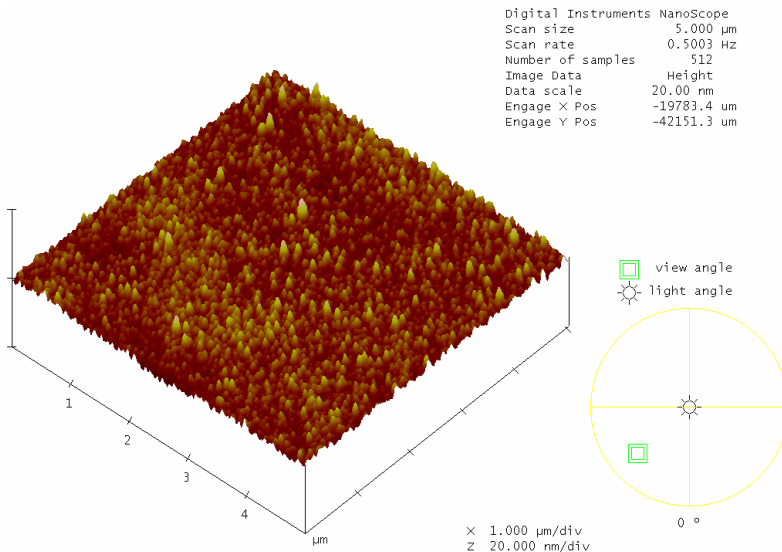


Fig. 7. Residual stress *versus* the aging time for $MgF_2/(SiN_x/SiO_2)^{22}$ quarter-wave stack.

thermore, the compressive stress changes to a tensile state of 4.82 MPa after the aging time of 168 hours, because the stress is released after deposition. Figure 7 shows a 45 layer $MgF_2/(SiN_x/SiO_2)^{22}$ QW stack which includes a MgF_2 film with high tensile stress. Stress evolution of this stack is very similar to that in Fig. 6. This result shows that the compressive residual stress is changed from -8.43 to -1.18 MPa, and after deposition of 168 hours, it changes to a tensile stress of 3.08 MPa. This difference is mainly due to the high tensile stress of the MgF_2 buffer layer to compensate for the compressive stress in the multilayer stacks [17, 18].



2015.08.25.011

Fig. 8. Surface roughness of SiN_x thin film measured by AFM.

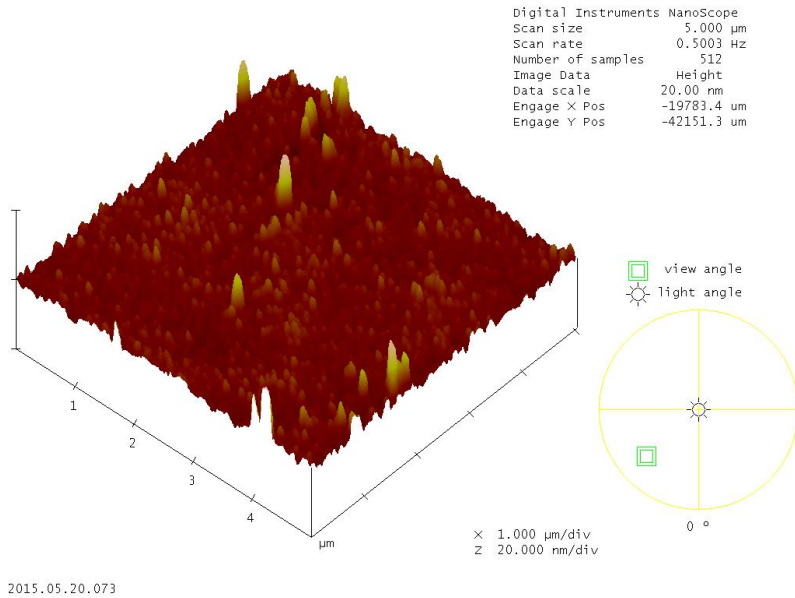


Fig. 9. Surface roughness of SiO₂ thin film measured by AFM.

The root mean square (RMS) of surface roughness (Rq) is a key parameter of thin film coatings. The surface roughness of a single layer is determined by the atomic force microscopy (AFM) and microscopic interferometer. Figure 8 reveals the 5 μm × 5 μm surface morphology of the SiN_x thin film with the surface roughness of 0.809 nm. Figure 9 shows the surface morphology of the SiO₂ thin film with the surface roughness of 1.330 nm which is higher than that of SiN_x single layer. The surface roughness of the

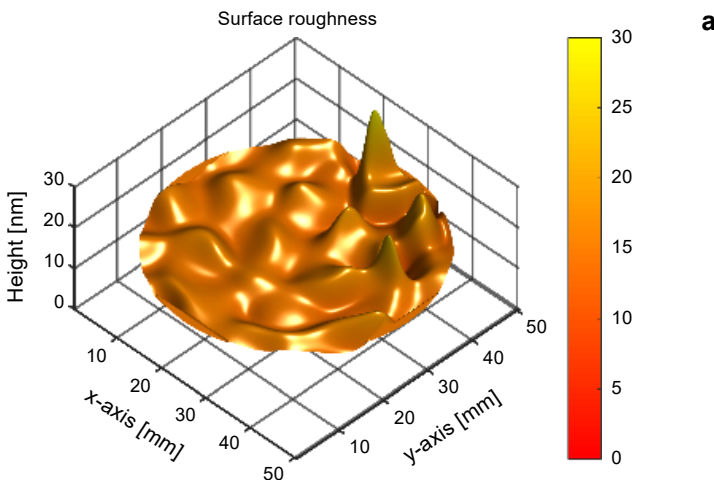


Fig. 10. Surface roughness of quarter-wave stacks (a) MgF₂/(SiN_x/SiO₂)²²; (b) (SiN_x/SiO₂)²² measured by a microscopic interferometer.

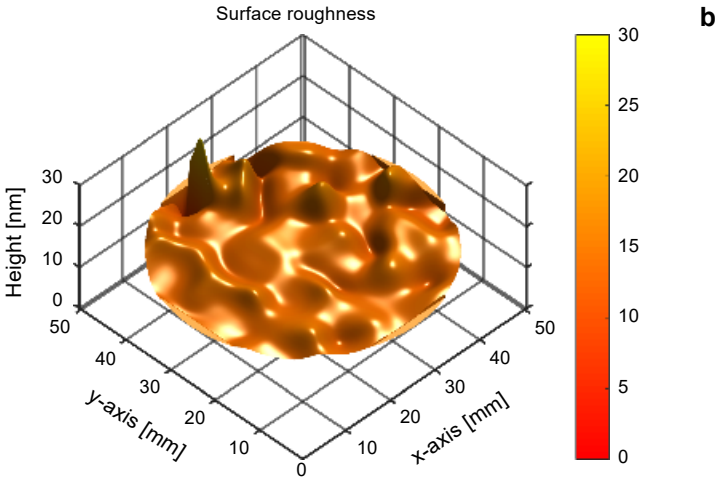


Fig. 10. Continued.

multilayer thin films was measured by a microscopic interferometer, and the measurement area was chosen for analysis in order to prevent any edge effects. Figure 10 shows the measurement results representing an actual dimension of $50\ \mu\text{m} \times 50\ \mu\text{m}$. The RMS surface roughness of $\text{MgF}_2/(\text{SiN}_x/\text{SiO}_2)^{22}$ and $(\text{SiN}_x/\text{SiO}_2)^{22}$ QW stack were 2.23 ± 0.22 and 2.08 ± 0.20 nm, respectively. The RMS surface roughness of sputtered $(\text{SiN}_x/\text{SiO}_2)^{22}$ film is slightly smaller than that of $\text{MgF}_2/(\text{SiN}_x/\text{SiO}_2)^{22}$ multilayer film. However, the latter structure design has a lower residual stress and smooth surface.

4. Conclusion

In this work, we investigated the effect of a MgF_2 buffer layer on the residual stress of $\text{SiN}_x/\text{SiO}_2$ quarter-wave stacks. The numerical simulation of multilayer stress behavior by using the MATLAB software was performed. It has been experimentally proved that stacking a buffer layer with tensile stress can effectively reduce the residual stress in the multilayer stacks. The main factors for the weight of the multilayer residual stress are the thickness of each layer, interface stress and the buffer layer design. The residual stress and aging effects in two different designs of $\text{SiN}_x/\text{SiO}_2$ multilayer films were measured by the FFT method. The aging effect of the two multilayer films was a function of exposure to air for 168 hours. The transition of two kinds of multilayer films changed from compressive stress to tensile stress over time. We also found that in the experiment of adding a MgF_2 film, it can reduce the residual stress in multilayer stacks through the balance of tensile and compressive stresses. It is possible to reduce the large compressive stress caused by sputtering process.

Acknowledgment – This work was supported by the Ministry of Science and Technology (MOST) of Taiwan under Grands MOST 104-2221-E-035-058-MY2 and 106-2221-E-035-072-MY2.

References

- [1] DUBEY R.S., JHANSIRANI K., SINGH S., *Investigation of solar cell performance using multilayer thin film structure ($\text{SiO}_2/\text{Si}_3\text{N}_4$) and grating*, Results in Physics **7**, 2017, pp. 77–81, DOI: [10.1016/j.rinp.2016.11.065](https://doi.org/10.1016/j.rinp.2016.11.065).
- [2] TIEN C.L., LIN T.W., *Thermal expansion coefficient and thermomechanical properties of SiN_x thin films prepared by plasma-enhanced chemical vapor deposition*, Applied Optics **51**(30), 2012, pp. 7229–7235, DOI: [10.1364/AO.51.007229](https://doi.org/10.1364/AO.51.007229).
- [3] JHANSIRANI K., DUBEY R.S., MORE M.A., SINGH S., *Deposition of silicon nitride films using chemical vapor deposition for photovoltaic applications*, Results in Physics **6**, 2016, pp. 1059–1063, DOI: [10.1016/j.rinp.2016.11.029](https://doi.org/10.1016/j.rinp.2016.11.029).
- [4] MENG X., BYUN Y.C., KIM H.S., LEE J.S., LUCERO A.T., CHENG L., KIM J., *Atomic layer deposition of silicon nitride thin films: a review of recent progress, challenges, and outlooks*, Materials **9**(12), 2016, article 1007, DOI: [10.3390/ma9121007](https://doi.org/10.3390/ma9121007).
- [5] ONG P.L., WEI J., TAY F.E.H., ILIESCU C., *A new fabrication method for low stress PECVD– SiN_x layers*, Journal of Physics: Conference Series **34**, 2006, pp. 764–769, DOI: [10.1088/1742-6596/34/1/126](https://doi.org/10.1088/1742-6596/34/1/126).
- [6] SRIDHAR N., RICKMAN J.M., SROLOVITZ D.J., *Multilayer film stability*, Journal of Applied Physics **82**(10), 1997, pp. 4852–4859, DOI: [10.1063/1.366347](https://doi.org/10.1063/1.366347).
- [7] ENNOS A.E., *Stresses developed in optical film coatings*, Applied Optics **5**(1), 1966, pp. 51–61, DOI: [10.1364/AO.5.000051](https://doi.org/10.1364/AO.5.000051).
- [8] TINONE M.C.K., HAGA T., KINOSHITA H., *Multilayer sputter deposition stress control*, Journal of Electron Spectroscopy and Related Phenomena **80**, 1996, pp. 461–464, DOI: [10.1016/0368-2048\(96\)03016-2](https://doi.org/10.1016/0368-2048(96)03016-2).
- [9] TAKEDA M., INA H., KOBAYASHI S., *Fourier-transform method of fringe-pattern analysis for computer-based topography and interferometry*, Journal of the Optical Society of America **72**(1), 1982, pp. 156–160, DOI: [10.1364/JOSA.72.000156](https://doi.org/10.1364/JOSA.72.000156).
- [10] TAKEDA M., MUTOH K., *Fourier transform profilometry for the automatic measurement of 3-D object shapes*, Applied Optics **22**(24), 1983, pp. 3977–3982, DOI: [10.1364/AO.22.003977](https://doi.org/10.1364/AO.22.003977).
- [11] TIEN C.L., ZENG H.D., *Measuring residual stress of anisotropic thin film by fast Fourier transform*, Optics Express **18**(16), 2010, pp. 16594–16600, DOI: [10.1364/OE.18.016594](https://doi.org/10.1364/OE.18.016594).
- [12] STONEY G.G., *The tension of metallic films deposited by electrolysis*, Proceedings of the Royal Society A **82**(553), 1909, pp. 172–175, DOI: [10.1098/rspa.1909.0021](https://doi.org/10.1098/rspa.1909.0021).
- [13] BRENNER A., SENDEROFF S., *Calculation of stress in electrodeposits from the curvature of a plated strip*, Journal of Research of the National Bureau of Standards (USA) **42**, 1949, pp. 105–123.
- [14] HSUEH C.H., *Modeling of elastic deformation of multilayers due to residual stresses and external bending*, Journal of Applied Physics **91**(12), 2002, pp. 9652–9656, DOI: [10.1063/1.1478137](https://doi.org/10.1063/1.1478137).
- [15] ZHANG X.C., XU B.S., WANG H.D., WU Y.X., *Optimum designs for multi-layered film structures based on the knowledge on residual stresses*, Applied Surface Science **253**(12), 2007, pp. 5529–5535, DOI: [10.1016/j.apsusc.2006.12.076](https://doi.org/10.1016/j.apsusc.2006.12.076).
- [16] YAHIA K.Z., *Simulation of multilayer antireflection coating for visible and near IR region on silicon substrate using MATLAB program*, Journal of Al-Nahrain University **12**(4), 2009, pp. 97–103.
- [17] KUPFER H., FLUGEL T., RICHTER F., SCHLOTT P., *Intrinsic stress in dielectric thin films for micro-mechanical components*, Surface and Coatings Technology **116–119**, 1999, pp. 116–120, DOI: [10.1016/S0257-8972\(99\)00114-0](https://doi.org/10.1016/S0257-8972(99)00114-0).
- [18] FLORO J.A., HEARNE S.J., HUNTER J.A., KOTULA P., CHASON P.E., SEEL S.C., THOMPSON C.V., *The dynamic competition between stress generation and relaxation mechanisms during coalescence of Volmer–Weber thin films*, Journal of Applied Physics **89**(9), 2001, pp. 4886–4897, DOI: [10.1063/1.1352563](https://doi.org/10.1063/1.1352563).